

1 **Geodynamical framework and hydrocarbon plays of a salt giant: the North**
2 **Western Mediterranean Basin**

3 **Pablo Granado^{1,2*}, Roger Urgeles³, Francesc Sàbat^{1,2}, Eduard Albert-**
4 **Villanueva^{1,4}, Eduard Roca^{1,2}, Josep Anton Muñoz^{1,2}, Nicoletta Mazzuca⁵ &**
5 **Roberto Gambini⁶**

6 ¹ *Institut de Recerca Geomodels, Universitat de Barcelona, Martí i Franquès s/n, 08028*
7 *Barcelona, Spain*

8 ² *Departament de Geodinàmica i Geofísica, Facultat de Geologia, Universitat de*
9 *Barcelona, Martí i Franquès s/n, 08028 Barcelona, Spain*

10 ³ *Departament de Geociències Marines, Institut de Ciències del Mar (CSIC), Pg.*
11 *Marítim de la Barceloneta, 37-49, 08003 Barcelona, Spain*

12 ⁴ *Departament de Geoquímica, Petrologia i Prospecció Geològica, Facultat de*
13 *Geologia, Universitat de Barcelona, Martí i Franquès s/n, 08028 Barcelona, Spain*

14 ⁵ *Enel S.p.A., viale Regina Margherita 137, 00198 Rome, Italy*

15 ⁶ *Enel Trade S.p.A., via Arno 42, 00198 Rome, Italy*

17 ** Corresponding author (e-mail: pablomartinez_granado@ub.edu)*

18 **Running title:** Geodynamical framework of a salt giant

19 **Abstract**

20 The North Western Mediterranean Basin developed during the Oligocene-
21 Miocene rifting of the Eastern Iberian-European magma-poor continental margin. The
22 margin developed as a result of back-arc extension associated with the roll-back of the

23 retreating Calabrian-Tethys subduction zone. Reinterpretation of 2D regional seismic
24 reflection data suggests that rifting took place by hyperextension of the Iberian-
25 European lithosphere. This process led to the seaward arrangement of distinct crustal
26 domains, namely proximal, necking and distal, whose distribution has been partly
27 controlled by the presence of transfer faults accommodating different amounts of back-
28 arc extension. **The late post-rift Messinian Salinity Crisis (MSC) gave place to**
29 **significant margin erosion and canyon incision whose lowstand sedimentary by-**
30 **products were largely deposited prior to the Messinian evaporitic sequences.**
31 Mesozoic-Cenozoic and Messinian to recent salt tectonics events have been recognized.
32 Such new understanding yields a distinct regional hydrocarbon play concept for
33 continental shelf to deep waters, including pre-salt, Messinian and post-salt plays.

34 **Key words:** *North Western Mediterranean Basin; Messinian Salinity Crisis; Crustal*
35 *hyperextension; Hydrocarbon plays.*

36 The North Western Mediterranean Basin is located between the Iberian-
37 European continental margin and its conjugate Corsica-Sardinia margin. It comprises
38 the Valencia Trough and the Balearic Promontory to the SW, and the Gulf of Lion and
39 the Provençal Oligocene-Miocene basins to the NE (Fig. 1). **The studied area displays**
40 **a well-developed shelf to slope and deep basin physiography with water depths in**
41 **excess of 2.5 km. Major shelf to slope depositional complexes are associated with**
42 **the Ebro and Rhone Rivers (Nelson & Maldonado, 1990; Evans & Arche, 2002;**
43 **Lofi *et al.*, 2003; Rabineau *et al.* 2014). The abyssal plain follows a NE-SW**
44 **trending bathymetric low that corresponds to the axis of the Provençal and**
45 **Algerian basins.** The Oligocene to Quaternary sedimentary infill ranges in thickness
46 from 2 to more than 6 km (Roca, 2001). **The North Western Mediterranean Basin is**
47 **characterised** by thin lithosphere ranging from 60 km beneath the Valencia Trough

48 axis to 30 km in the Provençal basin (Roca, 2001; Roca *et al.* 2004). **The regional**
49 **pattern of gravity and geoid anomalies suggest an asymmetric lithospheric**
50 **thinning across the Valencia Trough and towards the Provençal Basin (Ayala *et al.***
51 **1996, 2015). As to heat flow, data are sparse and unevenly distributed (see Roca *et***
52 ***al.* 2001 and Ayala *et al.* 2015 for a review), but existing surveys indicate a decrease**
53 **from 88 mWm⁻² at the SW termination of the Valencia Trough to 66 mWm⁻² in the**
54 **NE at the transition to the Provençal Basin, coincident with the deepest**
55 **bathymetry and thinnest crust (Foucher *et al.* 1992, Ayala *et al.* 2015). In the**
56 **central part of the Provençal Basin heat flow values seem to vary between 80-120**
57 **mWm⁻² in the southeast and 60-85 mWm⁻² in the northwest, with the highest**
58 **values occurring in the central parts of the basin (Pasquale *et al.* 1994).**

59 **Lithospheric thinning occurred in a continental crust that was formerly**
60 **consolidated during the Variscan orogeny. During the Mesozoic opening of the**
61 **Atlantic-Alpine Tethys oceans and the Bay of Biscay-Pyrenean rift, several**
62 **intracontinental extensional basins like the Columbretes, Maestrat and Cameros**
63 **basins developed in the Iberian Plate (Salas *et al.* 2001). During the Late**
64 **Cretaceous-Cenozoic shortening these Late Jurassic-Early Cretaceous extensional**
65 **basins were inverted and incorporated into the Alpine orogenic systems. Offshore**
66 **in the Valencia Trough, the Alpine shortening and related uplift is evidenced by a**
67 **large erosional truncation at the base of the Oligocene-Miocene sequence. It is**
68 **commonly accepted that the North Western Mediterranean Basin formed as a back-arc**
69 **basin in response to the roll-back of the African lithospheric slab, which was being**
70 **subducted beneath the Eurasian and Iberian plates along the retreating Calabrian-Tethys**
71 **subduction zone (Réhault *et al.* 1984; Doglioni *et al.* 1997; Lonergan & White, 1997;**
72 **Gueguen *et al.* 1998; Roca *et al.* 1999; Roca, 2001; Cavazza *et al.* 2004; Schettino &**

73 Turco, 2010; Jolivet *et al.* 2015). The northernmost part of the basin began to open
74 during the Oligocene, whereas the Algerian Basin to the South opened during the
75 middle Miocene (Sàbat *et al.* 1997). The main tectonic events and a synoptic
76 stratigraphy of the North Western Mediterranean Basin are summarised in figure 2.

77 **In our work, we have interpreted a large database of 2d regional seismic**
78 **profiles from the Valencia Trough and the Provençal Basin. A selection of relevant**
79 **examples is portrayed in figures 3, 4 and 5. These interpretations have been**
80 **integrated with lithospheric break up concepts (Brun & Beslier, 1996; Whitmarsh**
81 ***et al.* 2001; Lavier & Manatschal, 2006; Péron-Pinvidic *et al.* 2013) with the aim to**
82 **provide an updated geodynamic scenario and crustal architecture for the basin**
83 **(Figs. 1). This map of distinct crustal domains provides a geodynamic framework**
84 **for the Messinian Salinity Crisis (MSC), the observed salt-related structures and**
85 **finally, a hydrocarbon plays analysis. We want to remark the large extension of the**
86 **studied area and that the presented crustal architecture results, up to a certain**
87 **point, from a conceptual extrapolation for the entire basin.**

88 **Crustal domains of the North West Mediterranean Basin**

89 Hyperextension at “magma-poor” continental margins occurs when the ductile
90 part of the lithosphere is stretched to the point that its brittle parts become coupled,
91 allowing for large shear zones to penetrate into the mantle (Brun & Beslier, 1996;
92 Whitmarsh *et al.* 2001). **Stretching in such a way can lead to the exhumation of**
93 **lower crustal rocks and ultimately, to the exhumation and related serpentization**
94 **of the uppermost lithospheric mantle.** Such break-up processes are responsible for the
95 architectural organization of **magma-poor** continental margins and the seaward
96 arrangement of distinct crustal domains, namely proximal, necking, distal and outer.

97 **This architectural organization of crustal domains is mostly derived from studies**
98 **in the Atlantic continental margins (Whitmarsh et al. 2001; Lavier & Manatschal,**
99 **2006; Péron-Pinvidic et al. 2013). The proximal domain is characterised by fault-**
100 **bound sediment wedges belonging to graben or half-graben basins associated with**
101 **high angle or listric-shaped extensional fault systems. The necking domain displays**
102 **a wedge shaped crustal geometry, with the upwarping of the lower crust and**
103 **underlying Moho along major shear zones. The distal domain is fundamentally**
104 **shown by the occurrence of a sag basin developed over hyper-extended crust**
105 **and/or exhumed mantle as well as a shallow Moho. The outer domain in magma-**
106 **poor margins is rather difficult to map as it is shown as a gradual transition into**
107 **oceanic-type crust. At magma-rich margins, on the other hand, the presence of**
108 **voluminous volcanic and igneous complexes produces substantial crustal**
109 **thickening and related geophysical signatures (Péron-Pinvidic et al. 2013).**

110 From coastal Iberia to the Gulf of Lions, the western margin of the North
111 Western Mediterranean Basin is affected by Oligocene-Miocene NE-trending horsts and
112 grabens covered by a post-rift sedimentary wedge (Roca, 2001). A series of NW-SE-
113 trending system of transfer faults accommodated back-arc extension and have been the
114 loci of limited magma intrusion and lava extrusion from Aquitanian to Quaternary times
115 (Maillard et al. 1992). The **North Balearic Fracture Zone is one of these fault**
116 **systems and** separates the Provençal Basin, Gulf of Lions and their conjugate Corsica-
117 Sardinia margin to the **North** from the Valencia Trough, the Balearic Promontory and
118 the Algerian Basin to the **South** (Fig. 1b). Volcanic edifices and lava flows of Miocene
119 calc-alkaline and Pliocene alkaline affinity have been recognised on seismic data and
120 have also been drilled by several ODP/DSDP expeditions (Martí et al. 1992; Roca,
121 2001; Lofi et al. 2011a,b).

122 The Gulf of Lions is located on normal to slightly thinned crust belonging to
123 the proximal domain, whereas the Provençal Basin is characterised by a thick,
124 mostly Miocene to Plio-Quaternary sag basin that wedges out toward the Gulf of
125 Lions and the Balearic Promontory (Figs. 3 and 4). As first pointed out by Pascal *et*
126 *al.* (1992), the seismic velocities of the Provençal sag basin basement are arranged
127 in distinct domains neither typical of continental nor oceanic crust. Their
128 respective velocities are more consistent with lower continental crust, serpentinised
129 lithospheric mantle (Pascal *et al.* 1993; Bache *et al.* 2010; Jolivet *et al.* 2015) and
130 maybe, with an atypical thin oceanic crust affinity (Moulin *et al.* 2015). The
131 transition zone between the Gulf of Lions and the Provençal Basin has been
132 preliminary established based on the presence of lithospheric-scale shear zones
133 (i.e., expressed as the T and R crustal reflectors of Séranne *et al.* 1995), the
134 significant thinning of the crust away from the continent as well as the anomalous
135 seismic velocity field (Pascal *et al.* 1993; Gorini *et al.* 1993; Séranne *et al.* 1995;
136 Bache *et al.* 2010; Moulin *et al.* 2015). The transition from the proximal Gulf of
137 Lions into the distal domain corresponds to the necking domain (Figs. 1b, 3, 4).

138 A phase of subaerial erosion related with rift margin uplift has been
139 reported in the proximal and necking domains (Bache *et al.* 2010) and even in the
140 distal parts of the margin (Jolivet *et al.* 2015). This long-wavelength subaerial
141 erosion could relate to generalised rifting that initiated in Europe during the latest
142 Eocene and protracted during the Oligocene. The presence of thick fault-bounded
143 sediment wedges on the Provençal sag basin basement indicates graben and/or
144 half-graben basins developed on exhumed lower continental crust (Figs. 3). Based
145 on well (i.e., Golfe du Lion Profond 2 well – GLP2 – Guennoc *et al.* 2000) and
146 seismic data correlation, Jolivet *et al.* (2015) have recently proposed that these

147 sediment wedges could be as early as late Eocene in age. Jolivet *et al.* (2015) argue
148 that the seismic basement of the Provençal sag basin has been covered with
149 Eocene-Oligocene extensional wedges deposited onto exhumed lower continental
150 crust (i.e., syn-rift deposits) and lower Miocene wedges on exhumed lithospheric
151 mantle further outboard (i.e., syn-break up deposits). Strong uncertainties remain
152 regarding the age of these deposits as well as and their lateral correlation from the
153 proximal to the distal settings. It needs to be pointed out that the presence of these
154 distal rift to break-up basins is not clearly revealed by seismic data in all parts of
155 the studied area (compare Figs. 3 and 4). On the other hand, evidences of basement
156 extensional fault activity and volcanism in the necking domain during the middle
157 to late Miocene are present. As shown by seismic data, these major faults and
158 volcanic edifices may have controlled the subsequent distribution of evaporite
159 units during the Messinian Salinity Crisis (Fig. 4). All these observations indicate
160 the complexity of lithospheric break-up, but still suggest that it may have been a
161 diachronic process along the continental margin. This implies that break-up
162 sedimentation at the distal domain could have taken place in continental to marine
163 conditions.

164 **The distribution of crustal domains is more complex to the SW of the North**
165 **Balearic Fracture Zone separating the Provençal Basin from the Balearic**
166 **Promontory (Fig. 1b):** seismic reflection data indicates a thick Iberian lower crust,
167 whereas the whole extent of the Valencia Trough and the Balearic Promontory is
168 underlain by significantly-thinned lower crust (Sàbat *et al.* 1997; Roca, 2001; Ayala *et*
169 *al.* 2015). Along the axis of the Valencia Trough, the Moho rises gradually from 18-19
170 km at the SW end to just 8-10 km at the NE in the transition to the Provençal Basin
171 (Ayala *et al.* 2015). **The axis of the Valencia Trough can be considered a necking**

172 **zone with extremely thinned lower crust and a coupled upper crust and upper**
173 **lithospheric mantle.** Toward the SW termination of the trough, the Miocene
174 sedimentary fill was deposited on thinned Variscan continental crust overlaid by the **6-8**
175 **km thick Late Jurassic-Early Cretaceous Columbretes Basin (Fig. 5).** It is below
176 this Mesozoic basin that the upper crustal shear zones cross through the reflective lower
177 crust into the underlying lithospheric mantle (**Fig. 5**). **Crustal thickening associated to**
178 **the Betic fold-and-thrust belt development in the Balearic Promontory took place**
179 **coevally and after the main Oligocene to Miocene back-arc extensional stage, but**
180 **only affected the uppermost parts of the continental crust. In this sense, this**
181 **shortening has not restored the promontory's crust to its original pre-rifting**
182 **thickness as the lower crust was not involved (Sàbat *et al.* 1997; Roca, 2001).**
183 According to the above, the Balearic Promontory represents a crustal boudin
184 (Doglioni *et al.* 1997) or an H-Block (Peron-Pinvidic & Manatschal, 2010) between
185 the Valencia Trough necking zone and the distal domain represented by the
186 Algerian Basin (Fig. 1b).

187 **Sequence stratigraphy of the Messinian Salinity Crisis (MSC)**

188 From a seismic point of view 4 units have been traditionally ascribed to the
189 Messinian Salinity Crisis (see Lofi *et al.* 2011a,b; Bache *et al.* 2015 for recent
190 reviews): a lower unit corresponding to the Lower Evaporites, an intermediate
191 unit represented by the Mobile Unit (i.e., the megahalite body), and an upper unit
192 corresponding to the Upper Evaporites. At the base of the slope, a chaotic and
193 poorly imaged sedimentary body has also been recognized (Fig. 6) and mainly
194 interpreted as clastic deposits sourced from the margin. The Lower Evaporites and
195 Clastic Units have been grouped into a Messinian Lower Megasequence, whereas

196 the Mobile Unit and Upper Evaporites have been grouped into a Messinian Upper
197 Megasequence (Gorini *et al.* 2015).

198 Based on our observations and previously published works (Lofi *et al.*
199 2011b; Bache *et al.* 2015; Gorini *et al.* 2015; Urgeles *et al.* 2011; Granado *et al.*
200 2015; Cameselle & Urgeles 2016) we have addressed the MSC using a simple
201 sequence stratigraphic approach (Fig. 5) following the nomenclature provided by
202 Haq *et al.* (1987) and Posamentier *et al.* (1988). Before the MSC, a Tortonian-age
203 highstand systems tract (HST 1) is represented by prograding deltaic systems
204 (Figs. 2, 6a). The HST 1 is topped by a correlative conformity (*sensu* Posamentier
205 & Allen, 1999) that marks the sequence boundary (Fig. 6a). Then, the Messinian
206 sealevel drawdown and its associated margin incision lead to the partial erosion of
207 the former Tortonian deltaic system, the offlap and downlap of basinward-
208 stepping sedimentary systems represented by slope and basin floor fans belonging
209 to a lowstand systems tract (LST, Fig. 6b). This LST was characterized by high
210 progradation rates, fluvial erosion and incision on the marginal exposed areas, and
211 alluvial sedimentation on the slope and basin floor (Fig. 6b). This erosional surface
212 is marked by a subaerial unconformity (Fig. 6b), passing toward the basin into a
213 non-erosive maximum regressive surface. The transition point between this two
214 time-equivalent surfaces indicates the end of the base-level fall of the shoreline.
215 The LST deposits pass downslope and laterally into the earlier Lower Evaporites
216 succession, and should also include the Messinian Detritals described by Lofi *et al.*
217 (2011a,b), the U4 unit of Bache *et al.* (2015), the chaotic and imbricated units of
218 Cameselle & Urgeles (2016) or the Messinian Clastics of Gorini *et al.* (2015). The
219 high erosion and incision of the margin are responsible for the observed subaerial
220 unconformity that marks locally the sequence boundary (Fig. 6b). This subaerial

221 **unconformity should correspond to the Messinian Erosional Surface (MES)**
222 **described by many authors onshore and on the Mediterranean continental shelves**
223 **offshore (see Rouchy & Carusso, 2006; CIESM, 2008; Ryan, 2009; Urgeles *et al.***
224 **2011). However, an intense debate surrounds the origin of this unconformity. Some**
225 **authors postulate that the unconformity corresponds to sea-level still-stands (Lofi**
226 ***et al.* 2005), while others show evidence of a genesis of this surface during falling**
227 **sea level (Urgeles *et al.* 2011), and others argue that the latter stages of formation**
228 **where shaped during sea-level rise (Bache *et al.* 2009, 2012, 2015; García *et al.***
229 **2011). Extremely good preservation of fluvial deposits above the MES implies that**
230 **this erosional surface developed during sea level drawdown (Urgeles *et al.* 2011;**
231 **Cameselle *et al.* 2014).**

232 **Because the latest stage of reflooding of the basin has been estimated to**
233 **occur in a very short time span - some authors estimate that 90% of such**
234 **reflooding occurred in just 2 years (Garcia-Castellanos *et al.* 2009) - there is very**
235 **little to no evidence of a Pliocene transgressive systems tract. The retrogradational**
236 **and transgressive deposits, if at all present, are very thin in the Valencia Trough**
237 **(Cameselle & Urgeles 2016). Nevertheless, the onlap configuration of a large part**
238 **of the Lower Evaporites, the Mobile Unit and the Upper Evaporites in the**
239 **Provençal basin has been interpreted to result from initial slow Messinian**
240 **transgression (Bache *et al.* 2015). This transgressive systems tract (TST, Fig. 6c)**
241 **was likely characterized by continued, but reduced, clastic deposition. These**
242 **conditions gave way to the deposition of the later Lower Evaporites, the Mobile**
243 **Unit and the Upper Evaporites in a clearly transgressive context characterized by**
244 **the onlapping geometry of these units on to the early Messinian margin (Figs. 3, 4,**
245 **6c and 7a). Considerable controversy exists regarding the timing of deposition of**

246 the Mobile Unit (i.e., the megahalite body) and the Messinian Detritals. According
247 to Ryan (2009, 2011), salt deposition occurred early during the initial drawdown
248 and the formation of marginal and perched gypsum basins. Other authors like
249 Bache *et al.* (2009, 2015), Gorini *et al.* (2015) and Jolivet *et al.* (2015) assume that
250 the megahalite body was deposited later, more in agreement with our scenario
251 proposed above. In terms of relative age, this can be qualitatively assessed from
252 seismic profiles (Figs. 3 and 4), although poor seismic resolution hampers accurate
253 age estimation. We infer that the Messinian Clastic Units grade into the earliest
254 Lower Evaporites, although the latter are considered to be largely clastic in origin
255 too (Gorini *et al.* 2015). Precipitation of the late Lower Evaporites, the Mobile Unit
256 and the Upper Evaporites took place afterwards and more importantly, without
257 significant clastic sedimentation. In fact, the distribution of the Messinian
258 evaporitic units seems to have been controlled, at least to a certain degree, by the
259 inherited basement structure of the margin and volcanic edifices (Figs. 3 and 4).

260 Along the margin, the progradations belonging to the Plio-Quaternary HST
261 (i.e., HST 2, Figs. 2, 6d) of the Ebro and Rhone deltas directly downlap on the
262 Messinian Erosional Surface, whereas in the distal parts the Messinian evaporites
263 are overlain by biogenic oozes first and then by the distal deep water turbiditic
264 systems, roughly at the Plio-Quaternary transition (Cita, 1973; Bertoni &
265 Cartwright, 2005; Lofi *et al.* 2005; Kertznus & Kneller, 2009; Urgeles *et al.* 2011;
266 Rabineau *et al.* 2014). The maximum flooding surface between the top of the TST
267 succession and the base of the HST 2 deposits is located in the base of the biogenic
268 oozes, interpreted as a marine pelagic sedimentary unit deposited during the
269 maximum transgression (Fig. 6d).

270

271 **Salt tectonics in the North Western Mediterranean Basin**

272 **Salt tectonics in the North Western Mediterranean Basin is associated with**
273 **two salt-bearing units located in different sectors: the late Triassic salts in the the**
274 **Columbretes Basin within the Valencia Trough (Fig. 2) and the Messinian**
275 **megahalite body in the Provençal Basin (Figs. 3, 4, 7).** Well data in the Valencia
276 Trough indicate the Late Jurassic-Early Cretaceous Columbretes Basin is characterised
277 by a complete Mesozoic succession spanning from Triassic to Late Cretaceous times
278 (Lanaja, 1987) **with Late Triassic salt-bearing successions** (Fig. 2). As proven
279 onshore and offshore Iberia, the origin of the observed salt structures is related with the
280 Late Jurassic-Early Cretaceous rifting and their subsequent deformation during Alpine
281 shortening (Alves *et al.* 2003; Lopes *et al.* 2006; Ferrer *et al.* 2008; Roca *et al.* 2011;
282 Mencos *et al.* 2015). In the Columbretes Basin, **the salt-related structures are not**
283 **clearly evident due to the very poor seismic imaging, but hydrocarbon exploration**
284 **wells (Valencia 3-1 and Cabriel B-2A wells; Lanaja, 1987) drilled through Triassic**
285 **evaporites associated with structural highs bounding major Mesozoic depocenters.**
286 **The salt related structures correspond to diapirs and salt walls squeezed and**
287 **reactivated to different degrees (Martínez del Olmo, 1996).** Across the Valencia
288 Trough, the Messinian deposits are restricted to gypsum, carbonates and related clastic
289 units with no salt-bearing formations (Rouchy & Caruso, 2006; CIESM, 2008; Ryan,
290 2009; Lofi *et al.* 2011b; **Cameselle & Urgeles, 2016**). As a consequence, no salt
291 tectonics related to Messinian salts developed there.

292 **Conversely,** salt tectonics in the Provençal Basin is exclusively related to the
293 Messinian megahalite, which corresponds to the intermediate mobile unit originally
294 described by Montadert *et al.* (1978). Salt tectonics in the Provençal Basin is

295 represented by a well-developed gravity-driven system (Rowan *et al.* 2004). As other
296 world examples of gravity tectonics on continental margins salt basins, the Provençal
297 Basin system (**Figs. 3, 4 and 7**) is arranged in distinct salt-related domains: an updip
298 extensional belt, a translational belt and a down dip shortening belt (Dos Reis *et al.*
299 2008). The extensional belt (**Fig. 7a**) is characterised by regional listric faults and
300 associated hanging wall rollovers and footwall rollers (Sans & Sàbat, 1993); this system
301 is restricted updip by the stratigraphic pinch-out of the Messinian megahalite unit. The
302 topographic expression of volcanic edifices in the sag basin has affected the
303 development of the extensional belt and gravity tectonics along the margin in general
304 (Fig. 3). The translational domain is characterised by tabular salt, but it is not present all
305 across the basin; the shortening domain is constituted by buckle folds (**Fig. 4, 7b**),
306 diapirs and related salt structures (**Fig. 4, 7c**). **The distal salt structures show flanking**
307 **halokinetic sequences evidencing passive down building triggered by the Pliocene**
308 **to Quaternary Rhone deep sea fan systems sedimentation. As shown by the**
309 **halokinetic sequences, salt evacuation started as early as Messinian times**
310 **continuing today. Halokinetic sequence patterns suggest updip migration of**
311 **deformation as well, also indicated by the local absence of the tabular salt domain**
312 **(Fig. 3). Some diapiric structures show primary welds even if these diapirs pierce**
313 **or fold the sea bed. This is a clear indication that these structures are active, and**
314 **that either salt evacuation is still ongoing, and/or downdip shortening is taken**
315 **place (Fig. 7c).**

316 **Although still a question of debate in the studied area, the most accepted**
317 **mechanism for salt tectonics on continental margins is that gliding, spreading, or**
318 **both, take place in relation to the regional slope that post-rift differential thermal**
319 **subsidence generates. An interesting discussion on this matter has been provided**

320 by Rowan *et al.* (2004), Brun & Fort (2011, 2012), Rowan *et al.* (2012) and more
321 recently by Peel (2014). Sediment inputs from the continent (i.e., deltaic and deep
322 water) and subsidence can account for differential sedimentary loading, as an
323 additional but fundamental control for salt evacuation and inflation. In the
324 Provençal Basin, salt tectonics most probably resulted from a combination of
325 gliding and spreading and the downslope interaction with basement fracture zones
326 (Maillard *et al.* 2003; Dos Reis *et al.* 2008). The studied area is particularly
327 different to other salt giants like the Gulf of Mexico or the Central-South Atlantic
328 margins, where the salt units were deposited either during the syn-rift or the early
329 stages of post-rift. In the Provençal Basin, the Messinian Salt was regionally
330 deposited within an already well-established post-rift stage and, more importantly,
331 in a basin where no typical oceanic crust has been formed. Hence, there is no
332 Messinian salt deposited onto the basement/oceanic crust/exhumed mantle or
333 subsequently emplaced onto it. These differences have a strong impact on the
334 subsequent halokinetic history and structural styles developed. A regionally
335 deposited post-rift salt allows for a regional detachment surface along which post-
336 rift units can glide downslope, whereas the syn-rift half-graben restricted salts
337 form discontinuous horizons that hamper the gliding and rafting processes.

338 Different models to explain the observed large and delayed subsidence of
339 the Provençal sag basin have been proposed, including that of Réhault *et al.* (1984),
340 Séranne *et al.* (1999), and most recently Rabineau *et al.* (2014). According to
341 several authors (Bache *et al.* 2009, 2012; Ryan, 2011) the MSC sealevel drawdown
342 must have induced a large isostatic rebound of the rims of the North Western
343 Mediterranean Basin. This rebound was followed by significant but unevenly
344 distributed tilting and subsidence along the continental margin during the fast

345 **Zanclean reflooding (Rabineau *et al.* 2014). Govers *et al.* (2009) and Ryan (2011)**
346 **also propose that the loading imposed by the thick Messinian evaporites might**
347 **have contributed to the differential subsidence and tilting, triggering salt tectonics**
348 **in the Provençal Basin. According to Rabineau *et al.* (2014), the Plio-Quaternary**
349 **tilting of the margin and related basin subsidence is spatially arranged in a series**
350 **of distinct domains that we here assign to the proximal, necking and distal crustal**
351 **domains previously described (Fig. 1b). The updip extensional belt is spatially**
352 **coincident with the necking domain between the Gulf of Lions shelf and the**
353 **continental rise of the Provençal Basin. The necking domain displays a regional**
354 **slope into the deep sag basin that allowed for a potential energy differential that**
355 **triggered salt tectonics (Rowan *et al.* 2004; Hudec & Jackson, 2007; Brun & Fort,**
356 **2012; Peel, 2014). The translational and shortening domains are coincident with**
357 **the thickest part of the post-rift sag basin which developed on exhumed lower**
358 **continental crust, whereas the distalmost domain of diapirs is coincident with the**
359 **location of exhumed lower crust, serpentinised lithospheric mantle or atypical**
360 **oceanic crust.**

361 **Proven and speculative hydrocarbon plays**

362 Plays in the North Western Mediterranean Basin fall into two principal
363 categories: proven and speculative. In this work, shallow water vs. deep water and pre-
364 salt, Messinian and post-salt classification is proposed. Play types are summarized in
365 Table 1 and their location is schematically represented in a play concept diagram (**Fig.**
366 **8**). The sequential stratigraphic framework used corresponds to that presented here (**Fig.**
367 **6**) and is based on the pioneering work of Clavell & Berastegui (1991). The proven oil-
368 prone plays of the Valencia Trough (play 2, Table 1, **Fig. 8**) are preserved on

369 palaeohighs and tilted fault blocks (Clavell & Berastegui, 1991; Varela *et al.* 2005) on
370 the proximal domain. Main reservoir type is constituted by Aquitanian syn-rift
371 resedimented, fractured, karstified **and** dolomitised carbonate breccias and
372 conglomerates of various ages. These units are overlying the Mesozoic basement, which
373 is also fractured and karstified, and constitutes another reservoir type of less importance
374 (M. Esteban, pers. com. 2015). Hydrocarbon migration took place from the Jurassic
375 Ascla del Maestrat Formation and the Miocene Casablanca Shales (Fig. 2) updip and
376 across the extensional fault system (Clavell & Berastegui, 1991).

377 Speculative pre-salt plays are constituted by: Mesozoic basins on the necking
378 and proximal domains of the margin (play 1, **Figs. 3, 4, 8** and Table 1); Oligocene to
379 Miocene continental to marine wedges on the necking and distal domains of the sag
380 basin on top of significantly thinned crust and serpentinised mantle (play 3, Table 1,
381 Figs. 3, 8); Tortonian deltaic sandstones (play 4) and Tortonian deep sea fans (play 5)
382 belonging to the HST 1 (Figs. 3, **8** and Table 1). Messinian plays are constituted by:
383 slope and basin floor fans and mass transport deposits belonging to the **LST** (plays 6
384 and 7, **Figs. 6b, 8**; and Table 1) presently located in deep waters; fluvial sandstones
385 infilling the Messinian Erosional Surface (play 8) belonging to the **LST** in shallow
386 waters (Figs. 3, **6b and** Table 1). Post-salt plays are represented by: Pliocene-
387 Quaternary deltaic and shoreface sandstones (play 9) belonging to the HST 2 (Figs. 3, 4,
388 **6d, 8** and Table 1), probably charged with biogenic gas; Pliocene-Quaternary deep
389 water turbiditic sandstones belonging to the HST 2 trapped in rollovers of the gravity-
390 driven extensional domain (play 10, Figs. 3, **7a, 8** and Table 1), in channel/levee
391 systems (play 11, Figs. 3, 8 and Table 1) and in halokinetic sequences related with
392 diapirs and buckle folds of the gravity-driven shortening domain (play 12, Figs. 3, **7b,c**,

393 **8** and Table 1); pre- to syn-kinematic carbonates of the **Upper Evaporites** (play 13,
394 Figs. 3, **8** and Table 1).

395

396 **Conclusions**

397 **The North Western Mediterranean Basin shares certain stratigraphical and**
398 **structural similarities with prolific salt basins such as the South Central Atlantic,**
399 **but major differences exists regarding the timing of salt deposition as well as the**
400 **absence of a well-developed oceanic crust.** The conceptual evolutionary model
401 presented in this manuscript provides a geodynamic-architectural framework for
402 hydrocarbon exploration and has allowed defining a regional hydrocarbon play concept
403 diagram, where proven and speculative plays are summarized. **The MSC had a**
404 **profound effect on the Mediterranean margins' evolution in terms of subsidence,**
405 **burial, isostatic rebound and salt tectonics. The architectural organization of the**
406 **basin may have also controlled the distribution of the Messinian units, which**
407 **overall display a regionally transgressive character.** The effects of the MSC **has**
408 **provided** several potential source, reservoirs and seal horizons, in both shallow and
409 deep waters. In particular, the **LST** sedimentary bodies and erosional features
410 constituted multiple **reservoirs types and** stratigraphic and palaeogeographic traps.
411 These are **regionally sealed by prodelta shales on the shelf or by layered evaporites**
412 **sequences in the distal parts of the margin. Long-lived subsidence following rifting**
413 in the distal domain suggests the presence of thick source and reservoir intervals
414 overlying exhumed lower crust, and maybe, serpentinised lithospheric mantle.
415 Additionally, biogenic gas accumulations could be trapped in the shallow water
416 Pliocene deltaic systems.

417

418 **Acknowledgements**

419 This is a contribution of the Institut de Recerca Geomodels and the Geodinàmica
420 i Anàlisi de Conques research group (2014SGR467SGR) from the Agència de Gestió
421 d'Ajuts Universitaris i de Recerca (AGAUR) and the Secretaria d'Universitats i Recerca
422 del Departament d'Economia i Coneixement de la Generalitat de Catalunya. P.G.
423 acknowledges the financial support from ENEL Trade SpA (Project FBG307360) and
424 from the 'Grup de Recerca de Geodinàmica i Anàlisi de Conques', 2009 SGR 1198 of
425 the Comissionat d'Universitats i Recerca de la Generalitat de Catalunya. This work also
426 benefited from the financial support of SALCRETES (CGL2014-54118-C2-1-R)
427 project. ENEL Trade SpA is also thanked for permission to publish this research. Editor
428 Juan Soto and two anonymous reviewers are thanked for their constructive reviews on
429 original version of the manuscript. The "Archivo Técnico de Hidrocarburos" of the
430 Spanish "Ministerio de Industria y Comercio" provided the seismic data presented in
431 this study. We also thank IHS and Midland Valley which generously provided Kingdom
432 Suite and Move restoration software, respectively. Schlumberger is also acknowledged
433 for Petrel and Vista Educational and Research Licenses.

434

435 **References**

436 Alves, T. M., Gawthorpe, R. L., Hunt, D. H. & Monteiro, J. H. 2003. Post-Jurassic
437 tectono-sedimentary evolution of the Northern Lusitanian Basin (Western Iberian
438 margin). *Basin Research*, **15**, 227-249.

439 **Ayala, C., Pous, J. & Torne, M. 1996. The lithosphere-asthenosphere boundary of**
440 **the Valencia Trough (western Mediterranean) deduced from 2D geoid and gravity**
441 **modelling. *Geophysical Research Letters*, 23, 3131–3134 doi: 10.1029/96GL03005**

442 Ayala, C., Torne, M. & Roca, R. 2015. A review of the current knowledge of the crustal
443 and lithospheric structure of the Valencia Trough Basin. *Boletín Geológico y Minero*,
444 **126**, 533-552.

445 Bache, F., Olivet, J.L., Gorini, C., Rabineau, M., Baztan, J., Aslanian, D. & Suc, J.-P.
446 2009. Messinian erosional and salinity crises: View from the Provence Basin (Gulf of
447 Lions, Western Mediterranean). *Earth and Planetary Science Letters*, **286**, 139–157,
448 doi: 10.1016/j.epsl.2009.06.021.

449 Bache, F., Olivet, J. L., Gorini, C., Aslanian, D., Labails, C. & Rabineau, M. 2010.
450 Evolution of rifted continental margins: the case of the Gulf of Lions (Western
451 Mediterranean Basin). *Earth and Planetary Science Letters*, **3-4**, 345-356.

452 Bache, F., Popescu, S.-M., et al. 2012. A two-step process for the reflooding of the
453 Mediterranean after the Messinian Salinity Crisis. *Basin Research*, **24**, 125–153, doi:
454 10.1111/j.1365-2117.2011.00521.x.

455 **Bache, F., Gargani, J., Suc, J-P., Gorini, C., Rabineau, M., Popescu, S-M., Leroux,**
456 **E., Do Couto, D., Jouannic, G., Rubino, J-L, olivet, J-L., Cluzon, G., Dos Reis, A.T.**
457 **& Aslanian, D. 2015. Messinian evaporite deposition during sea level rise in the**
458 **Gulf of Lions (Western Mediterranean). *Marine and Petroleum Geology*, 66, 262-**
459 **277.**

460 Bertonni, C. & Cartwright, J. 2005. 3D seismic analysis of slope-confined canyons from
461 the Plio-Pleistocene of the Ebro Continental Margin (Western Mediterranean). *Basin*
462 *Research*, **17**, 43–62, doi: 10.1111/j.1365-2117.2005.00254.x.

463 **Brun, J.P. & Beslier, M.O. 1996. Mantle exhumation at passive margin. *Earth and***
464 ***Planetary Science Letters*, **142**, 161-173.**

465 **Brun, J.P. & Fort, X. 2011. Salt tectonics at passive margins: Geology versus**
466 **models. *Marine and Petroleum Geology*, **28**, 1123-1145.**

467 **Brun, J.P. & Fort, X. 2012. Salt tectonics at passive margins: Geology versus**
468 **models – Replay. *Marine and Petroleum Geology*, **37**, 195-208.**

469 Cameselle, A.L., Urgeles, R., De Mol, B., Camerlenghi, A. & Canning, J.C. 2014. Late
470 Miocene sedimentary architecture of the Ebro Continental Margin (Western
471 Mediterranean): implications to the Messinian Salinity Crisis. *International Journal of*
472 *Earth Sciences*, **103**, 423–440, doi: 10.1007/s00531-013-0966-5.

473 **Cameselle, A.L. & Urgeles, R. 2016. Large-scale margin collapse during Messinian**
474 **early sea-level drawdown: the SW Valencia trough, NW Mediterranean. *Basin***
475 ***Research* doi:10.1111/bre.12170**

476 Cavazza, W., Roure, F., Spakman, W., Stampfli, G. M. & Ziegler, P. A. (eds.) 2004.
477 The TRANSMED Atlas - The Mediterranean Region from Crust to Mantle. Springer,
478 Berlin-Heidelberg.

479 CIESM, 2008. The Messinian Salinity Crisis from mega-deposits to microbiology - A
480 consensus report. No. 33 in CIESM Workshop Monographs (F. Briand, Ed.), CIESM
481 Publisher, Monaco.

482 **Cita, M.B. 1973. Mediterranean evaporite: palaeontological arguments for a deep-**
483 **basin desiccation model. In: Messinian events in the Mediterranean**
484 **(Drooger, C.W. ed.), North-Holland Publ. Co, Amsterdam, pp. 206-228.**

485 Clavell, E. & Berastegui, X. 1991. Petroleum geology of the Gulf of Valencia. In: A. M.
486 Spencer (ed.). Generation, accumulation and production of Europe's hydrocarbons.
487 Special Publication of the European Association of Petroleum Geoscientists. No. 1,
488 335-368. Oxford University Press, The European Association of Petroleum
489 Geoscientists, Oxford.

490 Doglioni, C., Gueguen, E., Sàbat, F. & Fernández, M. 1997. The Western
491 Mediterranean extensional basins and the Alpine Orogen. *Terra Nova*, **9**, 109-112.

492 Dos Reis, A.T., Gorini, C., Weibull, W., Perovano, R., Mepen, M. & Ferreira, E. 2008.
493 Radial gravitational gliding indicated by sub-salt relief and salt-related structures: the
494 example of the Gulf of Lions, western Mediterranean. *Revista Brasileira de Geofísica*,
495 **26**, 347-365.

496 Evans, G. & Arche, A. 2002. The flux of siliciclastic sediment from the Iberian
497 Peninsula, with particular reference to the Ebro. In: Sediment flux to basins: causes,
498 controls and consequences (Jones, S.J. & Frostick, L.E. eds.), *Geological Society*,
499 *London, Special Publications*, **191**, 199–208.

500 Ferrer, O., Roca, E., Benjumea, B., Muñoz, J. A., Ellouz, N. & MARCONI Team. 2008.
501 The Deep seismic reflection MARCONI-3 profile: role of extensional Mesozoic
502 structure during the Pyrenean contractional deformation at the Eastern part of the Bay of
503 Biscay. *Marine and Petroleum Geology*, **25**, 714-730.

504 Foucher, J.E., Mauffret, A., Steckler, M., Brunet, M.E., Maillard, A., Réhault, J.E.,
505 Alonso, B., Deselgaux, E., Murillas, J. & Ouillon, G. 1992. Heat flow in the Valencia
506 trough: geodynamic implications. *Tectonophysics*, **203**, 77-97.

507 García, M., Maillard, A., Aslanian, D., Rabineau, M., Alonso, B., Gorini, C. & Estrada,
508 F. 2011. The Catalan margin during the Messinian Salinity Crisis: Physiography,
509 morphology and sedimentary record. *Marine Geology*, **284**, 158–174, doi:
510 10.1016/j.margeo.2011.03.017.

511 García-Castellanos, D., Estrada, F., Jiménez-Munt, I., Gorini, C., Fernández, M.,
512 Vergés, J. & De Vicente, R. 2009. Catastrophic flood of the Mediterranean after the
513 Messinian salinity crisis. *Nature*, **462**, 778–781, doi: 10.1038/nature08555.

514 Gorini, C., Le Marrec, A. & Mauffret, A. 1993. Contribution to the structural and
515 sedimentary history of the Gulf of Lions (western Mediterranean), from the ECORS
516 profiles, industrial seismic profiles and well data. *Bulletin Société Géologique de*
517 *France*, **164**, 353-363.

518 **Gorini, C., Montadert, L. & Rabineau, M. 2015. New imaging of the salinity crisis:**
519 **Dual Messinian lowstand megasequences recorded in the deep basin of both the**
520 **eastern and western Mediterranean. *Marine and Petroleum Geology*, **66**, 278-294.**

521 **Govers, R., Meijer, P. & Krijgsman, W. 2009. Regional isostatic response to**
522 **Messinian Salinity Crisis events. *Tectonophysics*, **463**, 109–129.**

523 Granado, P., Sàbat, F., Muñoz, J. A., Mazzuca, N., Griffi, G. & Gambini, R. 2015.
524 Traditional and new potential hydrocarbon plays in the NW Mediterranean. 77th EAGE
525 Conference and Exhibition – Workshops WS13 – Exploring the Mediterranean – New
526 Concepts related to the Messinian Salt. doi: 10.3997/2214-4609.201413563

527 Guennoc, P., Gorini, C. & Mauffret, A. 2000. Histoire géologique du Golfe du Lion et
528 cartographie du rift oligo-aquitain et de la surface messinienne, *Géologie de la*
529 *France*, **3**, 67–97.

530 **Gueguen, E., Doglioni, C. & Fernandez, M. 1998. On the post-25 Ma geodynamic**
531 **evolution of the western Mediterranean. *Tectonophysics*, **298**, 259-269.**

532 Hudec, M. & Jackson, M.P.A. 2007. Terra infirma: Understanding salt tectonics. *Earth-*
533 *Science Reviews*, **82**, 1-28.

534 **Haq, B.U., Hardenbol, J. & Vail, P.R. 1987. Chronology of fluctuating sea levels**
535 **since the Triassic (250 million years ago to present). *Science*, **235**, 1156-1166.**

536 Hunt, D. & Tucker, M. E. 1992. Stranded parasequences and the forced regressive
537 wedge systems tract: deposition during base-level fall. *Sedimentary Geology*, **81**, 1-9.

538 Jolivet, L., Gorini, C., Smit, J. & Leroy, S. 2015. Continental breakup and the dynamics
539 of rifting in back-arc basins: the Gulf of Lion margin. *Tectonics*, **34**, 662-679.
540 doi: 10.1002/2014TC003570.

541 Kertznus, V. & Kneller, B. 2009. Clinoform quantification for assessing the effects of
542 external forcing on continental margin development. *Basin Research*, **21**, 738–758, doi:
543 10.1111/j.1365-2117.2009.00411.x.

544 Lanaja, J. M. 1987. Contribución de la Exploración Petrolífera al Conocimiento de la
545 Geología de España, Instituto Geológico y Minero de España (IGME), Madrid.

546 Lavier, L. L. & Manatschal, G. 2006. A mechanism to thin the continental lithosphere at
547 magma-poor margins. *Nature*, **440**, 324-328

548 Lofi, J., Gorini, C., Berné, S., Clauzon, G., Dos Reis, A.T., Ryan, W.B.F. & Steckler,
549 M.S. 2005. Erosional processes and paleo-environmental changes in the Western Gulf

550 of Lions (SW France) during the Messinian Salinity Crisis. *Marine Geology*, **217**, 1–30,
551 doi: 10.1016/j.margeo.2005.02.014.

552 Lofi, J., Rabineau, M., Gorini, C., Berne, S., Clauzon, G., De Clarens, P., Dos Reis, T.,
553 Mountain, G., Ryan, W., Steckler, M & Fouchet, C. 2003. Plio–Quaternary prograding
554 cliniform wedges of the western Gulf of Lion continental margin (NW Mediterranean)
555 after the Messinian Salinity Crisis. *Marine Geology*, **198**, 289–317, doi: 10.1016/S0025-
556 3227(03)00120-8.

557 Lofi, J., Sage, F., Déverchère, J., Loncke, L., Maillard, A., Gaullier, V., Thinon, I.,
558 Gillet, H., Guennoc, P. & Gorini, C. 2011a. Refining our knowledge of the Messinian
559 Salinity Crisis records in the offshore domain through multi-site seismic arrays. *Bulletin*
560 *Société Géologique de France*, **182**, 163-180.

561 **Lofi J., Deverchère J., Gaullier V., Gillet H., Gorini C., Guennoc P., Loncke L.,**
562 **Maillard A., Sage F. & Thinon I. 2011b. Seismic atlas of the "Messinian Salinity**
563 **Crisis" markers in the Mediterranean and Black Seas. Commission for the**
564 **Geological Map of the World (CGMW), Mémoires de la Société Géologique de**
565 **France,179, 72 pp. 1 CD.**

566 Lonergan, L. & White, N. 1997. Origin of the Betic-Rif mountain
567 belt, *Tectonics*, **16** (3), 504–522, doi:[10.1029/96TC03937](https://doi.org/10.1029/96TC03937)

568 Lopes, F. C., Cunha, P. P. & Le Gall, B. 2006. Cenozoic seismic stratigraphy and
569 tectonic evolution of the Algarve margin (offshore Portugal, southwestern Iberian
570 Peninsula). *Marine Geology*, **231**, 1-36

571 Maillard, A., Mauffret, A., Watts, A.B., Torné, M., Pascal, G., Buhl, P. & Pinet, B.
572 1992. Tertiary sedimentary history and structure of the Valencia trough (western
573 Mediterranean). *Tectonophysics*, **203**, 57-75.

574 Maillard, A., Gaullier, V., Vendeville, B. C. & Odone, F. 2003. Influence of differential
575 compaction above basement steps on salt tectonics in the Calabrian-Provençal Basin,
576 northwest Mediterranean. *Marine and Petroleum Geology*, **20**, 13-27.

577 Martí, J., Mitjavila, J., Roca, E. & Aparicio, A. 1992. Cenozoic magmatism of the
578 Valencia trough (western Mediterranean): relationship between structural evolution and
579 volcanism. *Tectonophysics*, **203**, 145-165.

580 **Martínez del Olmo, W. 1996. Secuencias de depósito y estructuración diapírica en**
581 **el Mesozoico y Neógeno del Prebético y Golfo de Valencia desde sondeos y líneas**
582 **sísmicas. *Unpublished PhD Thesis. Universidad Complutense de Madrid. 503pp***

583 Mencos, J., Carrera, N. & Muñoz, J. A. 2015. Influence of rift basin geometry on the
584 subsequent post-rift sedimentation and basin inversion: the Organyà basin and the
585 Bóixols thrust sheet (South-Central Pyrenees). *Tectonics*, **34**,
586 doi:10.1002/2014TC003692.

587 Montadert, L., Letouzey, J. & Mauffret, A. 1978. Messinian event: seismic evidence. In:
588 K.J. Hsü, L. Montardert et al., In: Report of the DSDP, vol. XLII, part I, U.S. Govt.
589 Printing Office, Washington D.C., 1037-1050.

590 **Moulin, M., Klingelhofer, F., Afilhado, A., Schnurle, P., Rabineau, M., Berlier,**
591 **M.O. & Feld, A. 2015. Deep crustal structure across a young passive margin from**
592 **wide-angle and reflection seismic data (The SARDINIA Experiment) – I. Gulf of**
593 **Lion's margin. *Bulletin Société Géologique de France*, **186**, 309-330.**

594 Nelson, C.H. & Maldonado, A. 1990. Factors controlling late Cenozoic continental
595 margin growth from the Ebro Delta to the western Mediterranean deep sea. *Marine*
596 *Geology*, **95**, 419–440, doi: 10.1016/0025-3227(90)90127-6.

597 Pascal, G.P., Torne, M., Muhl, P., Watts, A.B. & Mauffret, A. 1992. Crustal and
598 velocity structure of the Valencia trough (Western Mediterranean). Part II Detailed
599 interpretation of five Expanded Spread Profiles. *Tectonophysics*, **203**, 21-35.

600 Pascal, G.P., Mauffret, A. & Patriat, P. 1993. The ocean-continent boundary in the Gulf
601 of Lions from analysis of expanding spread profiles and gravity modelling. *Geophysical*
602 *Journal International*, **113**, 701-726

603 **Pasquale, V., Verdoya, M. & Chiozzi, P. 1994. Types of crust in the Ligurian Sea.**
604 ***Terra Nova*, **6**, 255-266.**

605 Peel, F. J. 2014. The engines of gravity-driven movement on passive margins:
606 Quantifying the relative contribution of spreading vs. gravity gliding mechanisms.
607 *Tectonophysics*, **633**, 126-142

608 Péron-Pinvidic, G. & Manatschal, G. 2010. From microcontinents to extensional
609 allochthons: witnesses of how continents break apart? *Petroleum Geoscience*, **16**, 189-
610 197.

611 Péron-Pinvidic, G., Manatschal, G. & Osmundsen, P. T. 2013. Structural comparison of
612 archetypal Atlantic rifted margins: A review of observations and concepts. *Marine and*
613 *Petroleum Geology*, **43**, 21-47.

614

615 **Posamentier, H.W., Jervey, M.T. & Vail, P.R. 1988. Eustatic controls on clastic**
616 **deposition I – conceptual framework. In: Wilgus, C.K., Hastings, B.S., Kendall,**
617 **C.G.St.C., Posamentier, H.W., Ross, C.A. & Van Wagoner, J.C. (eds.). Sea Level**
618 **Changes – An integrated approach, Special Publication vol. 42. Society of**
619 **Economic Paleontologists and Mineralogists (SEPM) 1988, Tulsa, OK. USA, pp-**
620 **110-124.**

621 **Posamentier, H.W. & Allen, G.P. 1999. Siliciclastic sequence stratigraphy:**
622 **concepts and applications. Concepts in Sedimentology and Paleontology, vol. 7.**
623 **Society of Economic Paleontologists and Mineralogists (SEPM) 1999, Tulsa, OK.**
624 **USA, 210pp.**

625 **Rabineau, M., Leroux, E., Aslanian, D., Bache, F., Gorini, C., Moulin, M.m**
626 **Molliex, S., Droz, L., Dos Reis, A.T., Rubino, J.L., Guillocheau, F. & Olivet, J.L.**
627 **2014. Quantifying subsidence and isostatic readjustment using sedimentary**
628 **paleomarkers, example from the Gulf of Lion. *Earth and Planetary Science Letters,***
629 **388, 353-366.**

630 **Réhault, J.P., Mascle, J. & Boillot, G. 1984. Evolution géodynamique de la**
631 **Méditerranée depuis l'Òligocène. *Memorie della Società Geologica Italiana, 27, 85-***
632 ***96.***

633 **Roca, E. 2001. The Northwestern Mediterranean Basin (Valencia Trough, Gulf of Lions**
634 **and Liguro-Provençal basins): structure and geodynamic evolution. In: P.A. Ziegler, W.**
635 **Cavazza, A.H.F. Robertson & S. Crasquin-Soleau (Eds.). Peri-Tethyan Rift/Wrench**
636 **Basins and Passive Margins 186, 671-706. Peri-Tethys Memoir 6, Mémoires du**
637 **Museum National d'Histoire Naturelle, Paris.**

638 Roca, E., Sans, M. & Cabrera, L. 1999. Modelo tectonosedimentario del sector central y
639 septentrional del Margen Catalán sumergido (cubetas de Barcelona, Sant Feliu, Begur, y
640 Riumors-Rosas). In: Libro Homenaje a José Ramírez del Pozo. AGGEP, Madrid: 199-
641 217.

642 Roca, E., Frizon de Lamotte, D., Mauffret, A., Bracène, R., Vergés, J., Benaouali, N.,
643 Fernández, M., Muñoz, J. A. & Zeyen, H. 2004. TRANSMED Transect II. In: Cavazza,
644 W., Roure, F., Spakman, W., Stampfli, G.M. and Ziegler, P. (eds.). The TRANSMED
645 Atlas-The Mediterranean Region from Crust to Mantle. Springer, Berlin-Heidelberg.

646 Roca, E., Muñoz, J. A., Ferrer, O. & Ellouz, N. 2011. The role of the Bay of Biscay
647 extensional structure in the configuration of the Pyrenean Orogen: constraints from the
648 MARCONI deep seismic reflection survey. *Tectonics*, **30**, doi: 10.1029/2010TC002735,
649 2011

650 Rouchy, J. M. & Caruso, A. 2006. The Messinian salinity crisis in the Mediterranean
651 Basin: A reassessment of the data and an integrated scenario. *Sedimentary Geology*,
652 **188-189**, 35-67.

653 Roveri, M., Lugli, S., Manzi, V. & Schreiber, B.C. 2008. The Messinian Sicilian
654 stratigraphy revisited: new insights for the Messinian salinity crisis. *Terra Nova*, **20**,
655 483–488, doi: 10.1111/j.1365-3121.2008.00842.x.

656 Rowan, M. G., Peel, F. J. & Vendeville, B. C. 2004. Gravity-driven fold belts on
657 passive margins. In: K. R. McClay (ed.), Thrust tectonics and hydrocarbon systems.
658 AAPG Memoir **82**, 157-182.

659 **Rowan, M., Peel, F.J., Vendeville, B.C. & Gaullier, V. 2012. Salt tectonics at**
660 **passive margins: Geology versus models – Discussion. *Marine and Petroleum***
661 ***Geology*, 37, 184-194.**

662 Ryan, W. B., 2009. Decoding the Mediterranean Salinity Crisis. *Sedimentology*, 56, 95-
663 136.

664 **Ryan, W.B. 2011. Geodynamic responses to a two-step model of the Messinian**
665 **salinity crisis. *Bulletin de la Société Géologique de France*, 182 (2), 73-78.**

666 Sàbat, F., Muñoz, J. A. Vergés, J., Santanach, P., Masana, E., Sans, M., Estévez, A. &
667 Sasteban, C. 1997. Role of extensión and compression in the evolution of the eastern
668 margin of Iberia: the ESCI-València trough seismic profile. *Revista Sociedad Geológica*
669 *de España*, 8, 431-448.

670 Salas, R., Guimerà, J., Mas, R., Martín-Closas, C., Meléndez, A. & Alonso, A. 2001.
671 Evolution of the Mesozoic Central Iberian System and its Cenozoic inversion (Iberian
672 Chain). In: *Peri-Tethys Memoir 6: Peri-Tethyan Rift/Wrench Basins and Passive*
673 *Margins*. (eds. P.A. Ziegler, W. Cavazza, A.H.F. Robertson & S. Crasquin-Soleau).
674 Mém. Mus. natn. Hist. nat. 186, 145-185, Paris.

675 Sans, M. & Sàbat, F. 1993. Pliocene salt rollers and syn-kinematic sediments in the
676 northeast sector of the Valencia Trough (western Mediterranean). *Bulletin Société*
677 *Géologique de France*, 164, 189-198.

678 Schettino, A. & Turco, E. 2010. Tectonic history of the western Tethys since the Late
679 Triassic. *GSA Bulletin*, 123, 89-105.

680 Séranne, M., Benedicto, A., Labaume, P., Truffert, C. & Pascal, G. 1995. Structural
681 style and evolution of the Gulf of Lions Oligo-Miocene rifting: role of the Pyrenean
682 orogeny. *Marine and Petroleum Geology*, **12**, 809-820.

683 **Séranne, M. (1999). The Gulf of Lion continental margin (NW Mediterranean)**
684 **revisited by IBS: an overview. In: The Mediterranean Basins: Tertiary Extension**
685 **within the Alpine Orogen (Durand, B., Jolivet, L., Horvath, F., Seranne, M. eds.),**
686 ***Geological Society, London, Special Publication*, 156, 15–36.**

687 Urgeles, R., Camerlenghi, A., García-Castellanos, D., De Mol, B., Garcés, M., Vergés,
688 J., Haslam, I. & Hardman, M. 2011. New constraints on the Messinian sealevel
689 drawdown from 3D seismic data of the Ebro Margin, western Mediterranean. *Basin*
690 *Research*, **12**, 123-145.

691 Varela, J., Vicente-Bravo, J.C., Navarro, J., Esteban, M., Martínez del Olmo, W., 2005.
692 The Oil Fields in the Spanish Mediterranean Sea. In: *Asociación de Geólogos y*
693 *Geofísicos Españoles del Petróleo (AGGEP)* (ed. W. Martínez del Olmo). - XXV
694 Aniversario, 121-129.

695 Whitmarsh, R.B., Manatschal, G. & Minshull, T. A. 2001. Evolution of magma-poor
696 continental margins from rifting to seafloor spreading. *Nature*, **413**, 150-
697 154 doi:10.1038/35093085

698

699 **Figure list and captions**

700 **Figure 1. A)** Geographical setting of the North Western Mediterranean Basin. **B)**
701 Geological setting and onshore and offshore crustal domains of the studied area. The
702 Valencia Trough and the Balearic Promontory are underlain by significantly thinned
703 continental crust. **This regional map results from the integration of our**
704 **interpretations of available seismic data (SPBAL, RM, SGV, BG, VALSIS and**
705 **ECORS surveys) and previous works by Réhault *et al.* (1984), Pascal *et al.* (1992,**
706 **1993), Gorini *et al.* (1993), Séranne *et al.* (1995), Doglioni *et al.* (1997), Sábat *et al.***
707 **(1997), Lonergan & White (1997) Gueguen *et al.* (1998), Roca *et al.* (1999), Roca**
708 **(2001), Cavazza *et al.* (2004), Bache *et al.* (2010), Ayala *et al.* (2015), Granado *et al.***
709 **(2015) and Jolivet *et al.* (2015) Moulin *et al.* (2015). All these data were**
710 **conceptually extrapolated to the entire North Western Mediterranean Basin. AB:**
711 Algerian Basin; BP: Balearic Promontory; GOL: Gulf of Lion; VT: Valencia Trough.

712 **Figure 2.** Main tectonic events and synoptic stratigraphy of the studied area. PB:
713 Provençal Basin; VT: Valencia Trough; BP: Balearic Promontory. Based and modified
714 from Clavell & Berastegui (1991).

715 **Figure 3.** NW-SE trending seismic section SPBAL01_16 along the Provençal Basin.
716 **Significant outboard thinning of the crust is marked by the Moho upwarping and**
717 **the “T” and “R” reflections in the necking domain. Rift basins developed onto the**
718 **exhumed lower crust (ELC) of the distal domain. A volcanic edifice (V) is located**
719 **above the necking zone and has interacted with the gravity-driven system**
720 **associated to the Messinian salt. The intracrustal reflector is taken from Moulin *et***
721 ***al.* (2015). PQ: Pliocene-Quaternary; UE: Upper Evaporites; MU: Mobile Unit**
722 **(megahalite body); LE: Lower Evaporites; Tort: Tortonian; M Mio: middle**

723 **Miocene; Olig - L Mio: Oligocene to lower Miocene; Mz: Mesozoic Basin. UC:**
724 **Upper Crust; LC: Lower Crust. See figure 1b for location of the seismic profiles.**

725 **Figure 4. NE-SW trending seismic section SPBAL01_23 along the Provençal Basin.**
726 **Significant outboard thinning of the crust is marked by the “T” and “R”**
727 **reflections in the necking domain. Note the significant wedging of the sag basin**
728 **infill. The Lower Evaporites (LE) are clearly onlapping (see white arrow) and**
729 **wedging out onto the Balearic Promontory (BP). The Mobile Unit (MU) thins out**
730 **abruptly over a rift fault and a volcanic mound at the necking domain. The Upper**
731 **Evaporites (UE) are the extensive most Messinian unit onlapping further to the**
732 **SW onto the BP. PQ: Pliocene-Quaternary; Tort: Tortonian; V: Volcanics; Mz:**
733 **Mesozoic Basin; ELC: Exhumed Lower Continental Crust. See figure 1b for**
734 **location of the seismic profile.**

735 **Figure 5. WNW-ESE trending seismic section SGV01-107 along the Valencia Trough**
736 **and the Mesozoic Columbretes Basin. Note the significant thinning of the reflective**
737 **lower crust and its disappearance towards the ESE below a trans-lithospheric shear**
738 **zone. The strong erosion of the Mesozoic units below Oligocene to lower Miocene**
739 **strata provides evidence for the Alpine shortening and uplift. Miocene sediment**
740 **wedges, faulting and local uplift of this erosional surface evidences the Oligocene to**
741 **Miocene rifting of the Valencia Trough and coeval shortening of the Balearic**
742 **Promontory (see Fig. 2). Thin unconformable Messinian deposits are present in the**
743 **trough and have been buried by the prograding and aggrading Pliocene to Quaternary**
744 **delta system following post-Messinian flooding. T_R : Triassic salt diapir. See figure 1b**
745 **for location of the seismic profile.**

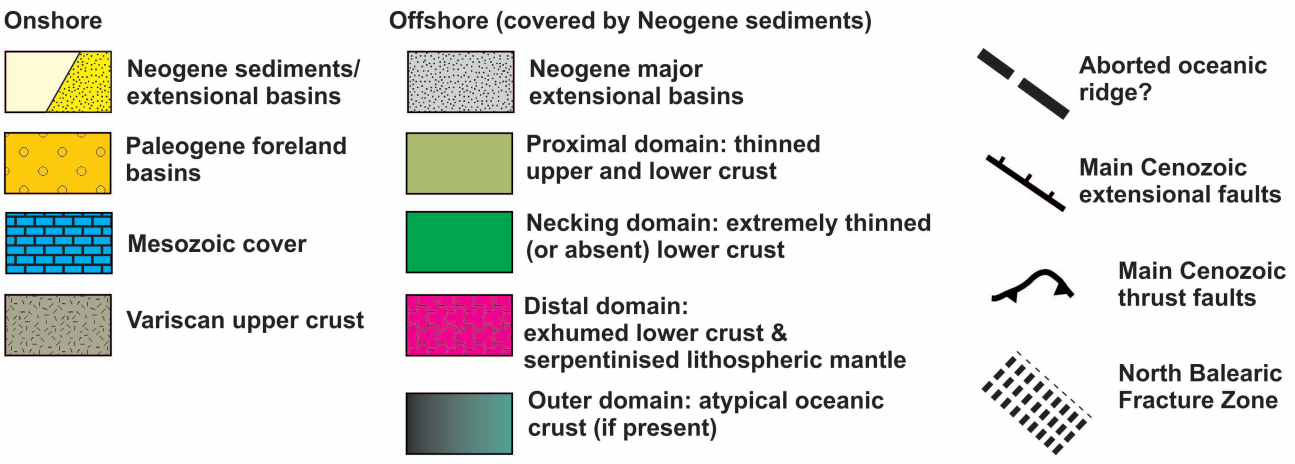
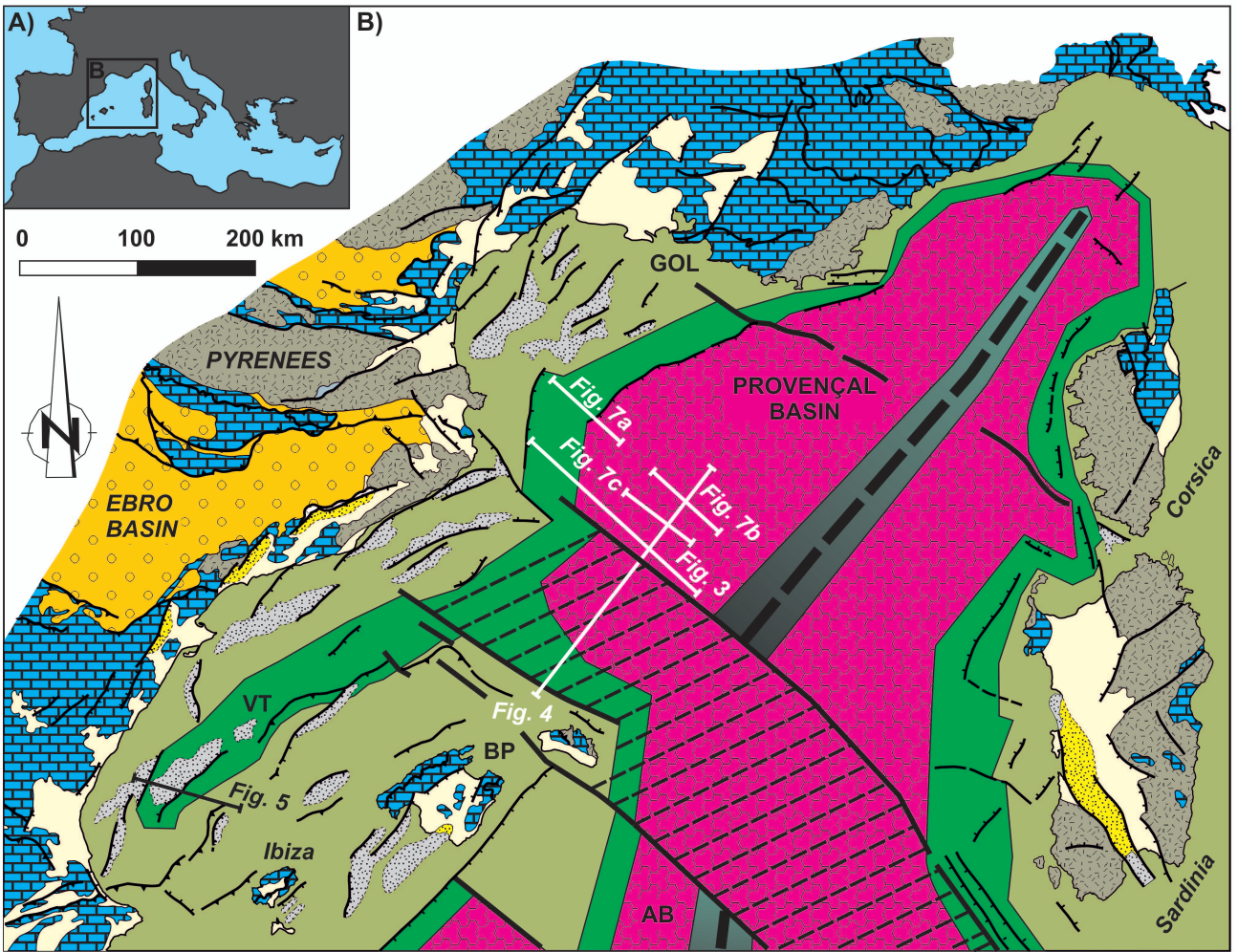
746 **Figure 6. Sequential stratigraphy of the Messinian Salinity Crisis proposed in this**
747 **study. A) Tortonian High Stand Systems Tract 1 (HST1). B) Messinian lowstand**
748 **systems tract (LST). C) Messinian transgressive systems tract (TST). D) Pliocene –**
749 **Quaternary High Stand Systems Track 2 (HST 2). Refer to the text for**
750 **explanations. Sequential stratigraphy terms refer to those by Haq *et al.* (1987),**
751 **Posamentier *et al.* (1988) and Posamentier & Allen, 1999.**

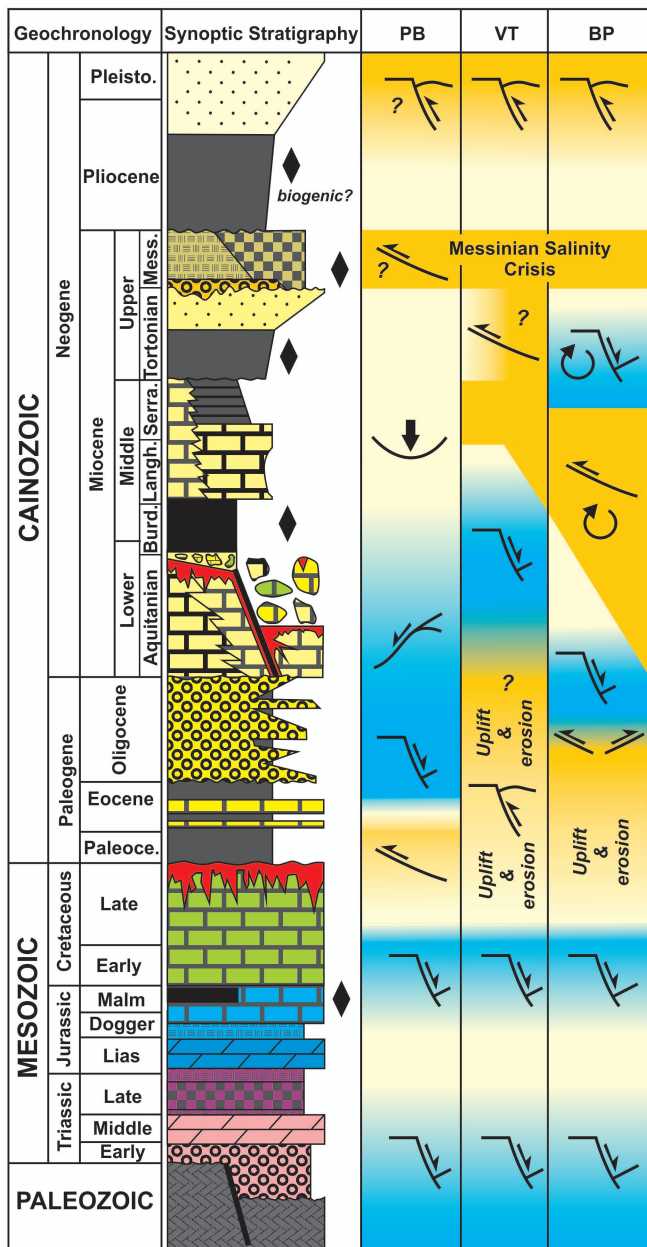
752 **Figure 7. Saline structures related with the Messinian salt (MU) in the Provençal**
753 **sag basin. A) SE-directed regional listric growth faults belonging to the extensional**
754 **domain of the gravity-driven system. These faults sole into the mobile unit and**
755 **have associated hanging-wall rollover folds and footwall salt rollers. Note how the**
756 **earlier Lower Evaporites (LE) pass laterally into the Messinian Detritals (MD),**
757 **whereas the late Lower Evaporites (LE) onlap onto these deposits. The mobile salt**
758 **unit thins toward the NW but it is still is on top of the Messinian Detritals. Taken**
759 **from seismic profile SPBAL01-04. B) Buckle folds of the shortening domain of the**
760 **gravity-driven system. Note the thickness changes of the Upper Evaporites and**
761 **along the Pliocene-Quaternary (PQ) succession indicating early but continued**
762 **evacuation of Messinian salt. Taken from seismic profile SPBAL01-04. C). Diapir**
763 **of Messinian salt in the distal domain of the gravity-driven system. The geometries**
764 **of the Pliocene-Quaternary halokinetic sequences associated to the diapir are also**
765 **indicative of early salt evacuation mostly by passive down building. Although**
766 **primary welds (i.e., black circles) at both sides of the diapir can be recognised, the**
767 **seabed is folded, suggesting the structure is actively growing either by being**
768 **sourced from outside the section or by being shortened. Taken from seismic profile**
769 **RM01_214. See figure 1b for location of the seismic profiles.**

770 **Figure 8.** Play concept diagram for the North Western Mediterranean Basin. The
771 diagram includes shallow to deep waters regions and conceptually integrates the
772 described crustal and salt-related domains and their respective prospective areas. See
773 text and table 1 for explanations.

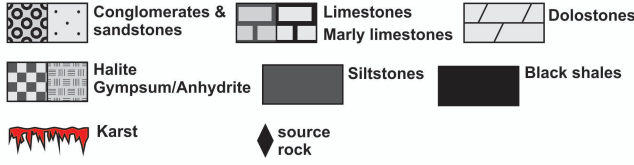
774 **Tables**

775 **Table 1.** Summary chart of North Western Mediterranean Basin plays.

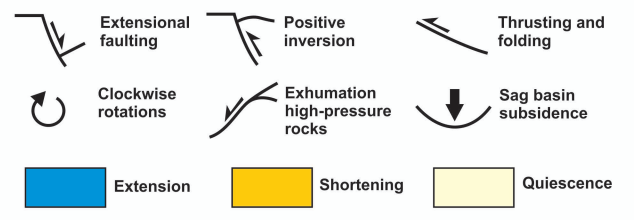


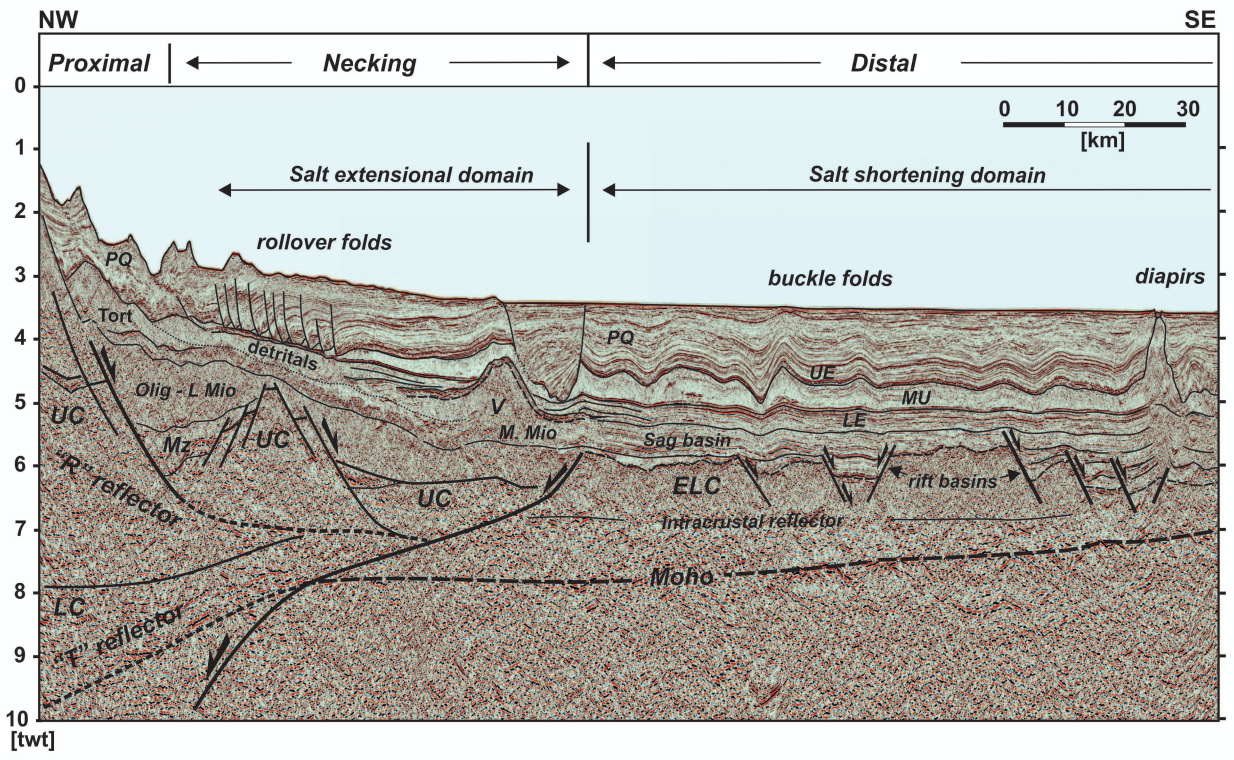


Stratigraphy



Tectonics





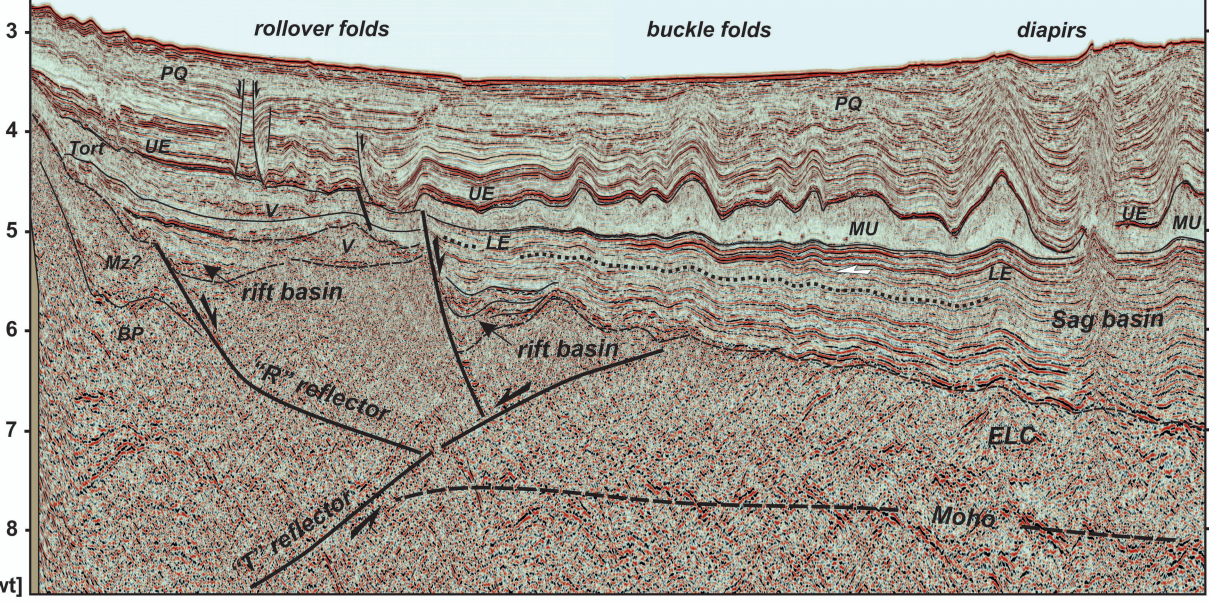
SW

NE

← Necking →
 ← Salt belts →
 ← Salt extensional domain →

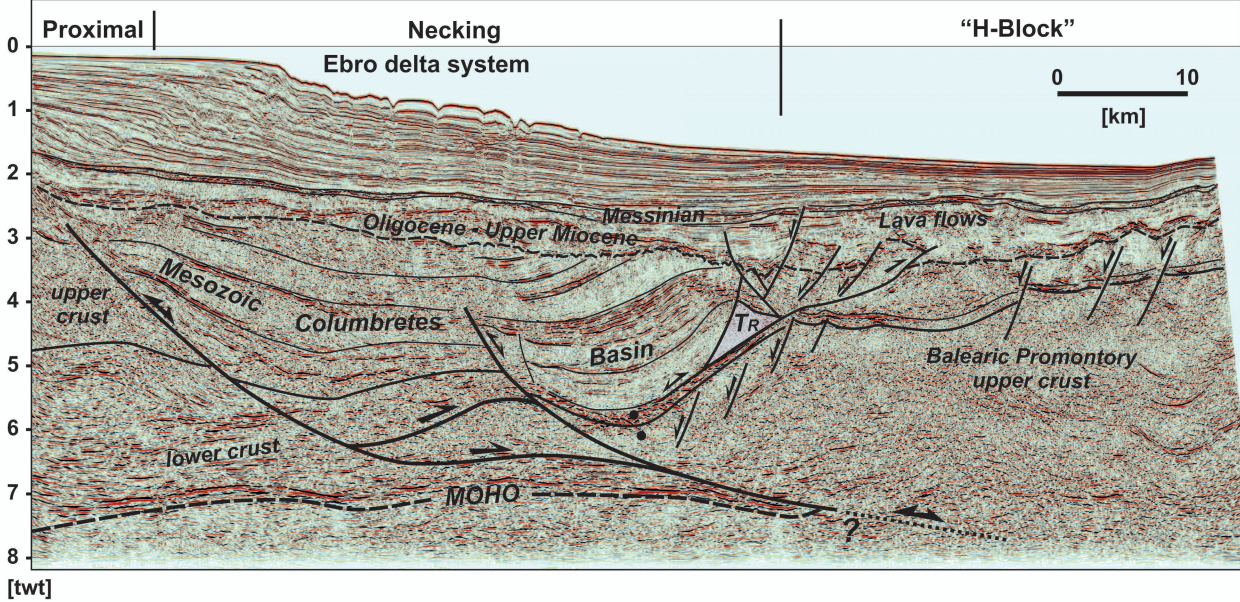
← Distal →
 ← Salt shortening domain →

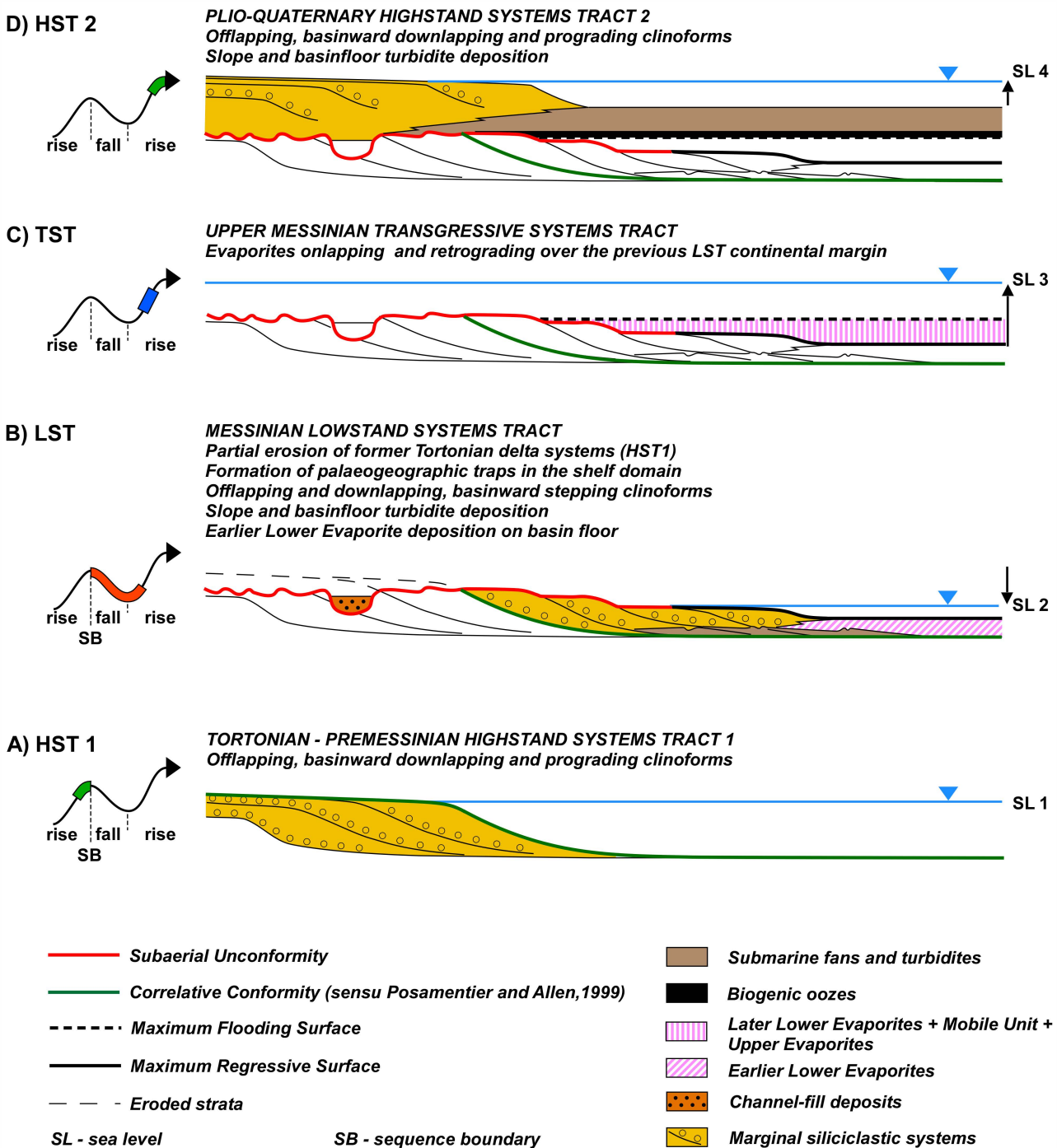
Crustal domains



WNW

ESE





HST - highstand systems tract TST - transgressive systems tract LST - lowstand systems tract

